CrossMark

SUITMA 8: SOILS AND SEDIMENTS IN URBAN AND MINING AREAS

Physical properties of structural soils containing waste materials to achieve urban greening

Deniz Yilmaz[1,2] · Patrice Cannavo[3,4] · Geoffroy Séré[5,6] · Laure Vidal-Beaudet[2,4] ·
Michel Legret[1] · Olivier Damas[7] · Pierre-Emmanuel Peyneau[1]

Abstract

Purpose The densification and expansion of urban areas will increase the streams of waste materials such as bricks, concrete and street sweeping waste. In parallel, green areas offer the potential to overcome many challenges that face growing/ expanding cities but require the use of large amounts of natural resources such as natural topsoil and aggregates. In this work, various waste materials mixed with organic debris are tested for greening applications in urban environments as an alternative to the consumption of natural resources.
Materials and methods Five combinations of artefacts were studied either as "growing material" (i.e. dedicated to plant growth) or "structural material" (as support for traffic). These constructed *Technosols* were studied in situ in lysimeters under two sets of contrasting climatic conditions at two sites in France (Angers, oceanic climate, and Homécourt semi-continental climate). They were planted with trees (*Acer platanoides*) and with ryegrass (*Lolium perenne* L.).

Results and discussion Compared to natural soils, the constructed Technosols exhibited high porosities and highly saturated hydraulic conductivities (up to 0.76 m³ m⁻³, and to 34.74 cm h⁻¹, respectively). The physical properties–i.e. macroporosity and microporosity–of these artificial soils revealed high water supply for plants, with available soil water ranging from 0.5 to 2.9 mm cm⁻¹. Tree and ryegrass roots were able to grow in the entire soil volume available in the lysimeters. Organic matter nature and soil pH conditions appeared to be the main drivers of plant development.
Conclusions Constructed Technosols are suitable for vegetation growth and constitute a valuable alternative to the consumption of natural arable earth for urban greening applications, e.g. gardens, parks, and tree lines. Furthermore, they can provide high levels of relevant ecosystem functions in cities such as water retention and infiltration, plant settlement, carbon sequestration and even biodiversity habitats.

Keywords Constructed *Technosols* · Roots · Soil hydraulic conductivity · Soil water availability · Soil water retention · Waste

✉ Pierre-Emmanuel Peyneau
   pierre-emmanuel.peyneau@ifsttar.fr

   Patrice Cannavo
   patrice.cannavo@agrocampus-ouest.fr

[1] LUNAM Université, IFSTTAR, GERS, EE,
   F-44340 Bouguenais, France

[2] Present address: Engineering Faculty, Civil Engineering Department,
   University of Tunceli, Tunceli, Turkey

[3] AGROCAMPUS OUEST, UP EPHOR, F-49042 Angers, France

[4] Université Bretagne Loire, Rennes, France

[5] Laboratoire Sols et Environnement, Université de Lorraine, UMR
   1120, TSA 40602, 54518 Vandoeuvre-lès-Nancy Cedex, France

[6] Laboratoire Sols et Environnement, INRA, UMR 1120, TSA 40602,
   54518 Vandœuvre-lès-Nancy Cedex, France

[7] Plante et Cité, 49066 Angers, France

1 Introduction

Vegetation has the potential to overcome many challenges facing cities over the coming decades, as caused by densification and expansion (Nielsen and Hansen 2007). The beneficial effects of plants in urban areas are multiple: we can mention benefits to humans (health, well-being), natural balance (biodiversity, temperature regulation, air quality, water infiltration and soil protection), and economy (plant waste recycling,

urban agriculture, territory attractiveness). In situ urban soils however very often lack the chemical and physical fertility and resistance to support plant growth (Morel and Schwartz 2005). Structural materials (also referred to as skeleton, stony or engineering soils, depending on the literature) are recognized as an alternative solution for preventing soil compaction in urban areas while limiting root penetration and plant growth. These materials consist of mixes of mineral soil and aggregates (around 10–40 mm in size) originating from quarries (Bartens et al. 2009; Grabosky et al. 2009). Such structural materials guarantee efficient water circulation (Grabosky et al. 2009; Novak et al. 2011), yet generally possess limited water availability for plant growth (Urban 2013); they also favor root anchorage and the structural stability of trees (Bartens et al. 2010).

Using topsoil from agricultural parcels for urban greening is currently controversial due to the decrease in arable surface area. An alternative idea for protecting these natural resources consists in reusing waste materials in order to construct functional soils (Séré et al. 2008). Cities are continuously being renewed through the demolition of older structures. This process produces demolition wastes, such as bricks, concrete, track ballast and excavated soils (Yuan and Shen 2011). These debris are regularly hauled outside of cities and only a fraction is being recycled (Marshall and Farahbakhsh 2013). In 2009 for instance, civil engineering activities were estimated to have generated 2.5×10^{11} kg of waste in France (ADEME 2012). Compost materials and green wastes stemming from garden and park maintenance are also generated within cities and massively exported out of urban areas to produce compost or energy. Some of these materials could be associated to build soils adapted to a multifunctional urban environment. Such soils have to be able to support plant growth, tree development and light traffic. As such, they need to display adequate bearing capacity, agronomic properties, drainage capacity and, moreover, must comply with environmental restrictions enforced to prevent pollutant release into the underlying aquifer (Craul 1999). The formulation of certain technogenic parent materials, associated in order to obtain mixtures specifically adapted to urban greening land uses, has already been studied by Rokia et al. (2014). The resulting mixtures can basically be divided into two categories: growing materials (high physical (i.e., water infiltration and soil water storage capacity) and chemical fertility), and structural materials (moderately fertile, with satisfactory bearing capacity and water drainage properties) (Grabosky et al. 2009).

At the urban scale and for rainwater management purposes, hydrodynamic properties are useful to model solute transfer, plant water supply and evapotranspiration in order to assess the ecosystem services provided by soils (Hanna et al. 2009; Djedjig et al. 2013). Despite their importance, the hydrodynamic properties of urban soils constructed with waste materials are rarely studied and remain somewhat obscure (Ojeda et al. 2011; Séré et al. 2012). Data for saturated hydraulic conductivity K_s in structural soils are scarce (Grabosky et al. 2009). Coarse constituents in soil are known to modify water transfer. Rock fragments may affect water storage (Ugolini et al. 1998; Sarah 2002; Tetegan et al. 2011), infiltration rate (Brakensiek and Rawls 1994; Cousin et al. 2003) and surface evaporation (Poesen and Lavee 1994). This paper is focused on the physical properties of soils, with an emphasis on the hydrodynamic properties of these formulated materials and resulting constructed soils.

The purpose of the present study is twofold: (1) to assess the transposition of natural soils methods to characterize the physical properties of artificial growing and structural materials with methods used for natural soils and (2) to evaluate the capacity of some vegetation types to grow in these materials. Thus, the suitability of constructing structural soils with wastes and by-products instead of arable soil and aggregates for urban greening is assessed.

2 Materials and methods

2.1 Materials

The processes of waste selection, collection and sampling have been described elsewhere (Rokia et al. 2014). During a pedological engineering project intended to construct soils in urban areas, a total of 11 wastes was selected from the European waste catalogue (European Commission no. 94/3/EC 1993). The selection criteria were production volume, availability throughout French regions, low toxicity, and potential fertility as mineral and/or organic constituents for soil construction.

The growing material (GM) was a mixture of 58 wt.% of brick manufacturing waste and 42 wt.% of a compost made of sewage sludge and green wastes. Four mixtures were considered as structural materials; they were all based on the association of an excavated earth material from a deep horizon with a coarse mineral material (natural or artefact) and an organic material (natural or artefact) (Table 1). Chemical characteristics of fine soil (<2 mm) of GM and SM are presented in Table 2.

2.2 Experimental set-up

For practical reasons, two experimental sites were used for the study of the different artificial structural soils. The sites were contrasted in terms of experimental systems (2 m³ lysimetric column and 0.5 m³ lysimetric containers). Indeed, each lysimetric device was adapted to the vegetation type and development.

Table 1 Origin and composition of the structural materials (SM)

| Name | Earth material | Mineral coarse material | | Organic material | |
	Weight ratio	Origin	Weight ratio	Origin	Weight ratio
SM-Control	0.27	Chalcedony	0.70	Leaf mold	0.03
SM-BS	0.20	Track ballast	0.76	Sewage sludge	0.04
SM-CG	0.32	Concrete waste	0.65	Green wastes	0.03
SM-RG	0.22	Demolition rubble	0.75	Green wastes	0.03

2.2.1 Lysimeter at the Homécourt site (GISFI, France, 49° 12′ N 5° 59′ E)

A 2-m deep, 1-m² surface area lysimeter installed at the GISFI experimental station (http://www.gisfi.fr) in Homécourt (northeastern France), supplied by Umwelt-Gerate-Technik (Müncheberg, Germany), was filled with the parent materials in October 2012 (see Fig. 1). A 15-cm sand bed was placed at the bottom to ensure homogeneous drainage. The structural material was SM-CG. The technogenic materials were gradually added and manually compacted every 30 cm. No water table was applied. The lysimeter was subjected to atmospheric conditions. The climate was continental with a mean annual temperature of 10 °C and a mean annual precipitation of 763 mm. The soil was sown with ryegrass (*Lolium perenne L*. var. *Tove*) at a density of 240 kg ha^{-1}. One replicate was studied, as previous studies demonstrated the validity of the hydrodynamic and vegetation development monitoring over a long period of time without replicates (Séré et al. 2012; Huot et al. 2015).

2.2.2 Lysimeters at the Angers site (Agrocampus Ouest, France, 47°28′ N 0°36′ W)

Nine 0.480-m³ lysimeters, along with three copies of three distinct constructed soils, were built at the Angers (France) Agrocampus in April 2013 and then subjected to atmospheric conditions (Fig. 2). The climate was temperate with a mean annual temperature of 12 °C and a mean annual precipitation of 650 mm. The growing material was set in a 0.025-m³ cylinder at the center of the lysimeter and surrounded by some of the structural material. A tree was planted in the growing material (*Acer platanoides*) of each lysimeter. The structural material was SM-Control for three lysimeters, SM-BS for three others and SM-RG for the remaining three lysimeters. Each year, one replicate was destroyed for soil and tree growth characterization.

2.3 Measurement methods

The Technosols considered herein contained coarse elements (centimeter-sized fragments of brick or concrete can easily be spotted) and therefore required adapted protocols to characterize their behavior.

Table 2 Chemical characteristics of the fine soil (<2 mm) of the materials

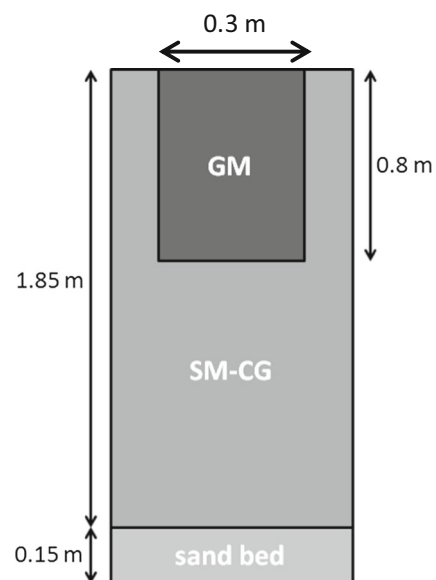|	OM (g kg^{-1})	Total N (g kg^{-1})	C/N	pH H$_2$O	CEC (cmol + kg^{-1})
GM	271.0	17.0	9.3	7.0	42.9
SM-Control	62.4	2.0	18.2	4.6	14.3
SM-BS	48.1	3.4	8.1	6.7	11.1
SM-CG	40	1.5	15.7	8.2	15.1
SM-RG	23.4	0.9	14.9	7.7	4.1
	CaO (g kg^{-1})	P$_2$O$_5$ (g kg^{-1})	K$_2$O (g kg^{-1})	MgO (g kg^{-1})	Na$_2$O (g kg^{-1})
GM	13.3	0.8	4.3	1.8	0.6
SM-Control	4.0	0.2	0.4	0.5	0.1
SM-BS	3.6	0.2	0.2	0.3	0.1
SM-CG	16.3	0.07	0.3	0.3	0.2
SM-RG	15.1	0.1	0.5	0.2	0.2

Organic matter (OM), NF ISO 14235 (1998); Total N, NF ISO 13878 (1998); pH, NF ISO 10390 (2005); CEC, NF X 31-130; CaO, K$_2$O, MgO, Na$_2$O NF X 31-108; Olsen phosphorus, NF ISO 11263 (1995)

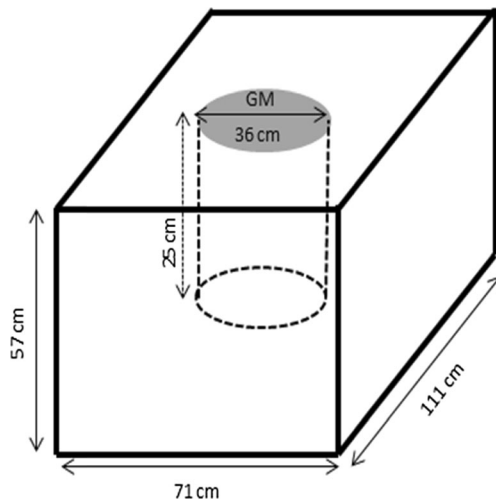**Fig. 1** Lysimeter design at the GISFI site

Fig. 2 Lysimeter design at the Agrocampus Ouest site

2.3.1 Density and total porosity

Initial dry bulk density (ρ_d) of the materials was determined by weighing them when filling lysimeters. Thereafter, it was estimated by measuring material packing and based on the new volume of material. Particle density (ρ_s) was measured based on the NF P94-054 (1991) standard method. Then, total porosity φ (v/v) was calculated using Eq. 1:

$$\varphi = 1 - \frac{\rho_d}{\rho_s} \qquad (1)$$

2.3.2 Water infiltration

Tension disk infiltration experiments were conducted to estimate in situ hydrodynamic properties using an 8-cm-diameter minidisk infiltrometer (Decagon Devices, Pullman, WA, USA). These experiments were performed in June 2014 in Homécourt and Angers sites and in June 2015 in Angers site only. This method has already proven to be reliable for stony soils (Baetens et al. 2009). Disk infiltrometer devices have been developed to characterize hydrodynamic properties. The infiltration data collected from such experiments can be inversed using numerical models (Mallants et al. 1997; Šimůnek et al. 1998; Schwartz and Evett 2002; Ramos et al. 2006; Kodesova et al. 2010; Yilmaz et al. 2013) in order to retrieve the soil hydrodynamic parameters.

A thin layer of Fontainebleau sand, characterized by a particle size distribution ranging between 0.2 and 0.3 mm along with highly saturated hydraulic conductivity was applied to optimize contact between the disk membrane and the material. The sand was moistened immediately before placing the disk membrane onto the material surface in order to further improve contact and prevent air from entering the disk (Cameira et al. 2003). These infiltration experiments were

conducted at negative pressure heads of −5, −3, −1 and 0 cm on the lysimeter.

Before each infiltration experiment, one sample was collected using a circular ring to measure the initial water content. The samples were oven-dried at 105 °C for at least 48 h. Moreover, dry bulk dry density was calculated at the lysimeter surface. Measurements in the materials were performed in duplicate.

Both soil water retention $h(\theta)$ and soil unsaturated hydraulic conductivity $K(\theta)$ curves were obtained by inverting multi-tension disk infiltration data using the HYDRUS 2D/3D software program (Šimůnek et al. 2008). HYDRUS is able to simulate water movement in variably saturated porous media: this software program numerically solves the Richards equation governing the flow thanks to a finite element approximation. For the inversion of infiltration data, HYDRUS uses the Levenberg-Marquardt inversion algorithm (Marquardt 1963). This nonlinear least-squares method yields a vector of parameters that minimizes the distance between specific measurements and the corresponding model predictions. HYDRUS is frequently implemented to model water infiltration experiments (Šimůnek and van Genuchten 1996, 1997; Ramos et al. 2006; Šimůnek et al. 2008). The dimension of the numerical flow domain, i.e. 40 cm by 40 cm, is large enough to represent the moisture front below the infiltration device. Finite elements of 2 mm in length were chosen to discretize the numerical domain. The upper boundary condition corresponds to the imposed pressure head under the device, and zero flux boundary conditions were applied elsewhere.

2.3.3 Hydrodynamic parameters

Van Genuchten-Mualem (Mualem 1976; Van Genuchten 1980) models are classically used to describe the hydrodynamic functions $h(\theta)$ and $K(\theta)$:

$$\frac{\theta - \theta_r}{\theta_s - \theta_r} = \left(1 + \left(\frac{h}{h_g}\right)^n\right)^{-m} \qquad (2)$$

$$m = 1 - \frac{1}{n} \qquad (3)$$

$$K(\theta) = K_s \left(\frac{\theta - \theta_r}{\theta_s - \theta_r}\right)^l \left[1 - \left(1 - \left(\frac{\theta - \theta_r}{\theta_s - \theta_r}\right)^{1/m}\right)^m\right]^2 \qquad (4)$$

where n and m are the dimensionless hydrodynamic shape parameters that depend on material texture, l is a dimensionless parameter and h_g (L), θ_s (L^3 L^{-3}), θ_r (L^3 L^{-3}) and K_s (LT^{-1}) are the hydrodynamic scale parameters that depend on material structure. θ_s and θ_r are the saturated and residual water contents, respectively, h_g the scale parameter for the water pressure head, K_s the saturated hydraulic conductivity and l the pore connectivity parameter (usually set at 0.5).

The residual water content θ_r was set at 0.05 for all materials. Numerical simulations actually revealed that the precise value of the residual water content did not affect inversion results provided it was set at less than or equal to 0.1. Total porosity φ was used to estimate saturation $\varphi = 1 - \frac{\rho_d}{\rho_s}$.

2.3.4 Soil particle size distribution

Samples collected in situ to estimate the initial water content before infiltration experiments were used to determine the particle size distributions. After drying, all samples were sieved through a 80-μm sieve. The standard method NF EN 933-1 (2012) was used for the fraction greater than 80 μm and a laser particle size analyzer (Malvern Mastersizer 3000) for the fraction smaller than 80 μm (in accordance with the standard NF X 11-666).

2.3.5 Soil air and water availability

The soil hydrodynamic parameters were used to assess air and water availability in order to evaluate the physical properties of such artificial soils constructed from waste materials.

Available soil water (ASW) was calculated as follows:

$$ASW\ (v/v) = \theta_{fc} - \theta_{wp} \tag{5}$$

where θ_{fc} is the volumetric water content at field capacity (in $m^3\ m^{-3}$), and θ_{wp} the volumetric water content at the wilting point ($m^3\ m^{-3}$).

θ_{fc} and θ_{wp} were obtained from soil water retention curves at 3.16 and 160 m, respectively. Air availability was estimated from the macroporosity MP (v/v) calculation using the following equation:

$$MP = \theta_s - \theta_{fc} \tag{6}$$

2.3.6 Vegetation development

In October 2014, the lysimeter from the GISFI site was dismantled and root distribution was examined. The method was based on an in situ mapping protocol described by Tardieu and Manichon (1986), with a regular grid (2 cm × 2 cm cells); root occurrence was defined by a colored cell and its absence by an empty cell.

In June 2014 and 2015, three lysimeters from the Agrocampus Ouest site, corresponding to the SM-Control, SM-BS and SM-RG mixtures, were dismantled. At first, the tree aerial part was cut at the soil surface level. Leaves, shoots and the trunk were separated, and dry weights were determined after drying at 65 °C for 1 week. The root biomass distribution was derived according to the Böhm (1979) method. Each lysimeter was divided into three layers (I, II, III), each with the same thickness (Fig. 3), and each divided into nine cubic blocks of the same volume (ranging between 0.014 and 0.017 m^3 depending on the lysimeter). A total of 27 blocks was defined for each lysimeter, from which the roots were manually extracted. These blocks were washed with distilled water, then dried at 65 °C for 1 week and weighed. Root density was calculated in each block by dividing root biomass by block volume.

2.3.7 Statistical analysis

Both the mean difference and correlation significance were tested using R software (R Core Team 2015). Root mean square errors (RMSE) were calculated for each infiltrometer experimental inversion in order to assess inversion quality. Assuming a normally distributed noise, the confidence intervals were defined by applying Gaussian theory to a linearization around the Levenberg-Marquardt estimate (Seber and Wild 2003).

3 Results

3.1 Soil physical properties

3.1.1 Particle size distribution

Particle size distribution (PSD) analysis, involving manual sieving and supplemented by a grain size analysis, is illustrated in Fig. 4 for both the growing and structural materials. The function F represents the cumulative percentage passing at diameter D. The particle size distribution of artificial structural materials was comparable for particle sizes varying from 0 to 10 mm, even though SM-CG exhibited a higher proportion of 0.01-to-0.5 mm fraction. SM-BS and SM-CG however displayed higher particle size fractions from 10 to 30 mm (30 %) than SM-Control and SM-RG (5 %), whereas SM-Control and SM-RG presented higher coarse materials from 30 to 80 mm (60 %) than SM-BS and SM-CG (23 %). The growing material had a distinctly higher proportion of 0.5-to-20 mm fraction compared to SMs.

3.1.2 Bulk density, solid density and total porosity

Dry bulk density ρ_b, specific density ρ_s and total porosity of each material are listed in Table 3. GM had the lowest specific and dry bulk densities and thus a higher total porosity value, i.e. between 0.68 and 0.76 $m^3 \cdot m^{-3}$. SM can be divided into two groups. SM-CG and SM-RG had similar specific density values, while their dry bulk density values were less than 1.5 $g\ cm^{-3}$. SM-Control and SM-BS have higher specific density values, higher dry bulk density values and lower total porosity values. The total porosity of SM ranged from 0.31 to 0.48 $m^3\ m^{-3}$, 1.5 to 2.3 times smaller than the mean total porosity of the growing material.

Fig. 3 Root sampling design in each lysimeter
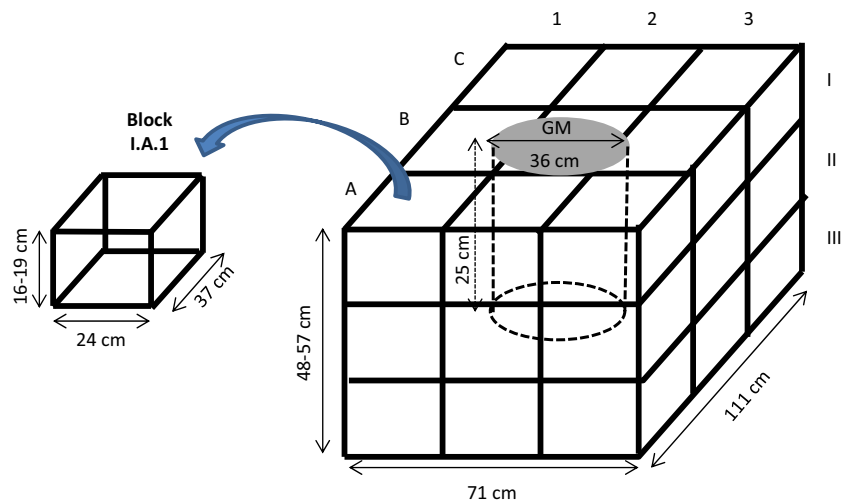
3.2 Hydraulic properties

3.2.1 Multi-tension disk infiltration and inversion method

Figure 5 shows the multi-tension disk infiltration experiment data points for the GM material at both the Homécourt and Angers sites. The hydrodynamic parameters proposed for sand material in the HYDRUS database were used as initial parameters for the inverse procedure.

Experimental infiltration curves displayed four relatively straight portions with increasing slopes in absolute value terms. Each portion corresponded to a given suction applied on the material surface (starting from −5 cm, then −3, −1 and 0 cm): as suction approached zero, the water saturation of the material increased, resulting in higher hydraulic conductivity and a higher infiltration rate.

The model proposed through this inversion procedure fitted the experimental data quite well. RMSE values were

between 3.4 and 5.1 cm^3. The GM of Angers site systematically indicated lower water infiltration than Homécourt for a given infiltration time.

Figure 6 depicts the multi-tension disk infiltration experiment (through its points) performed on SMs at both sites. Once again, the model fitted the experimental data very well. RMSE values were between 1.1 and 6.5 cm^3. Various curve patterns can be observed depending on SM type as well as on replicate number. A high variability in the replicates was also observed for SM-BS and SM-Control. It should be noted however that total infiltration as a function of time was a cumulative quantity and, as such, became more sensitive to even slight variations in the hydrodynamic parameters over time.

3.2.2 Hydrodynamic parameters

The hydrodynamic parameters of GM are shown in Table 4. Due to high organic matter content, the values of saturated

Fig. 4 Particle size distribution of GM (*closed black squares*), SM-CG (*open grey squares*), SM-BS (*open grey diamonds*), SM-Control (*gray crosses*) and SM-RG (*open grey triangles*)
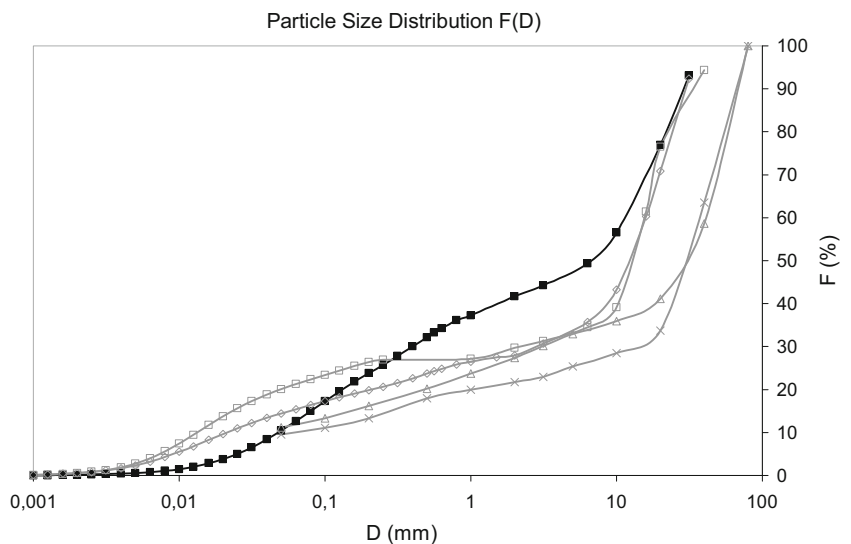
Table 3 Samples, initial and saturated volumetric water contents, dry bulk and specific densities of the materials

Treatment	Dry bulk density ρ_b (g cm^{-3})	Solid density ρ_s (g cm^{-3})	Total porosity φ (m^3 m^{-3})
GM Homécourt site	0.70	2.18	0.68
GM Angers site	0.53		0.76
SM-Control	1.81	2.63	0.31
SM-BS	1.78	2.69	0.36
SM-RG	1.46	2.51	0.42
SM-CG	1.29	2.50	0.48

water content were high (with a mean of 0.73). The average value of parameter n equaled 1.57 for Homécourt and 1.48 for Angers. The estimated saturated hydraulic conductivity K_s fell in the same range, i.e. 31.0 cm h^{-1} for Homécourt, and 26.4 cm h^{-1} for Angers. The capillary length h_g was twice as small at Angers. In fact, the denser the material, the longer the capillary since the typical pore size is reduced by means of compaction, thus leading to an increase in capillary length. Besides, no significant evolution of hydrodynamic parameters was noted in the Angers site between 2014 and 2015 (Table 4).

The hydrodynamic parameters of SM in 2014 are given in Table 5. As opposed to GM, θ_s of SM-Control was very low (0.31) as, to a lesser extent, so was SM-BS (0.36), which turned out to be comparable to a silty clay soil. The saturated water contents were higher in SM-RG (0.42) and SM-CG (0.48). The saturated hydraulic conductivity values ranged from 2.6 to 9.5 cm h^{-1}, which indicates that these materials were semi-permeable media. K_s for SM-RG was significantly

higher than SM-BS and SM-CG ($p < 0.01$). Parameter h_g also posted heterogeneous values. Similar observations can be drawn from a close inspection of the hydrodynamic parameters obtained for other SMs. In particular, capillary length values differed considerably, for both SM-BS and SM-Control. When compared to the growing material, the parameter n of SM was significantly lower, with a mean value of 1.20 and standard deviation of 0.1 ($p < 0.001$). The mean K_s values (5.6 cm h^{-1}) for SM were 5 times as low ($p < 0.01$) and capillary length h_g was averaged at 13.5 cm, which is twice as high ($p < 0.01$) as the corresponding average value for the growing material. In 2015, a significant increase in K_s was observed whatever the SM is ($p < 0.1$) (Table 5), with a mean value of 24.7 cm h^{-1} (i.e. comparable to K_s for GM in 2015, Table 3).

Soil water retention curves $h(\theta)$ derived from average Van Genuchten parameters calculated for each 2014 material are presented in Fig. 7. These curves reflect distinct patterns for GM and SM. In particular, GM had a higher saturated water content (0.73 v/v) than SMs (between 0.31 and 0.48 v/v). Soil water retention curves varied slightly from one SM to another. Despite an overall shape analogous to coarse-textured soils, residual water (i.e. water at high water potential) was surprisingly high (0.11 v/v). The unsaturated conductivity (K) curves derived from the average Van Genuchten parameters calculated for each material are presented in Fig. 8a (vs. water content) and Fig. 8b (vs. matric potential) for 2014 only. Compared to GM, and except for SM-BS, the unsaturated hydraulic conductivity curves of the other SMs featured very similar patterns and were comparable to those of a sandy soil. When matric potential was near 0 cm (i.e. soil water saturation), hydraulic conductivity was almost 100 times as high in GM as in SMs. This difference remained the same when matric

Fig. 5 Multi-tension disk infiltration experiments conducted on GM at GISFI in Homécourt and in Angers; *symbols* represent experimental data points and the *solid lines* are fits with optimized parameters
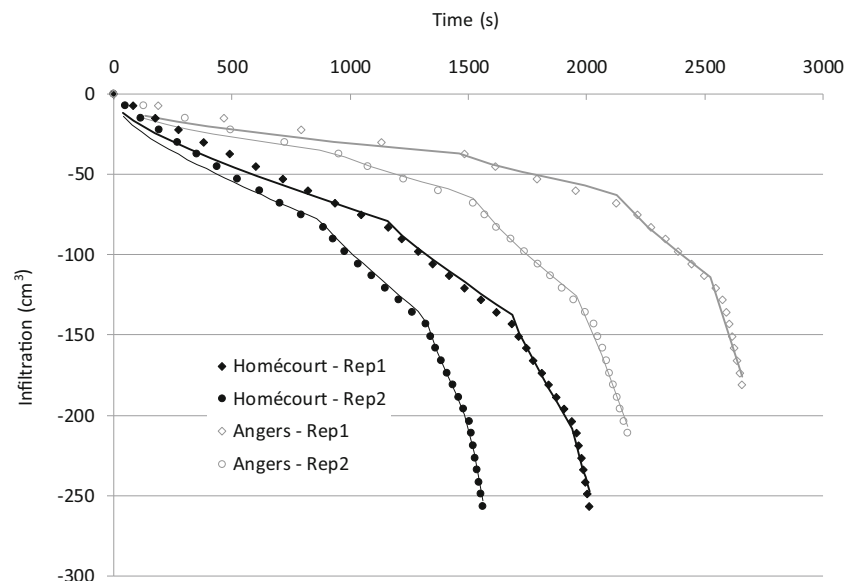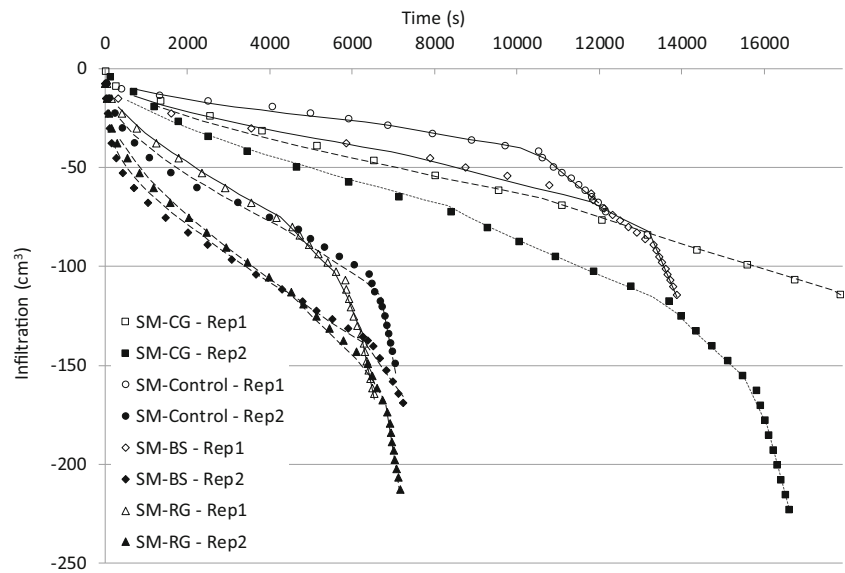
Fig. 6 Multi-tension disk infiltration experiments conducted on structural materials. The *symbols* represent experimental data and lines for fits corresponding to optimized parameters

potential was near 316 cm (i.e. soil water field capacity), except for the hydraulic conductivity of SM-BS which was only 3.7 times lower than that of GM.

3.2.3 Evaluation of physical properties

MP and ASW in 2014 and 2015 are presented in Table 6. In 2014, GM offered the highest ASW (3 mm cm^{-1}, which was 3.6 to 5.6 times as high as in SM materials, $p < 0.05$). GM also consistently had higher mean MP (0.31 v/v) than SMs ($p < 0.05$). Considering SMs, MP was particularly low in SM-BS (lower than 0.1 v/v) and was within the same range as SM-Control. In 2015, there were no significant differences in ASW, except for GM and SM-RG whose ASW values respectively decreased and increased ($p < 0.05$). Similarly, no significant change was observed in MP.

Assuming actual evapotranspiration of 5 mm day^{-1} in summer without any rainy days (Meteo France database for both sites), the time-lapse required for vegetation to reach water stress conditions was estimated. Considering the Angers site lysimeters in 2014, GM accounted for a water stress delay of 15.5 days (volume of material 25 L), whereas all SMs presented comparable values around 6.3 days (volume of material

455 L). The highest water stress delay for SMs was found at the Homécourt site, with SM volumes almost 4 times as high. In 2015, water stress delay changed significantly for SM-RG, with a 1.4-fold increase ($p < 0.05$).

3.3 Development of vegetation

3.3.1 Trees

Tree root densities are listed in Table 7. In 2014, both SM-Control and SM-RG had comparable total root densities, measuring 1.3 10^{-3} and 1.0 10^{-3} v/v (volume of root per volume of material), respectively. Total root density in SM-BS was reduced by 30 % compared to other treatments. As expected, the highest root density was found in the growing material (GM), with a mean density of 1.6 10^{-2} v/v in block I.B.2. Root density was lowest in the deepest layer; compared to layer I, it stood at 3.6, 10.1 and 2.9 times as lower in the SM-Control, SM-BS and SM-RG treatments, respectively. Total root biomass equaled 550, 278 and 424 g dw in the same three sample treatments, respectively, among which 80, 79.5 and 73.3 % were ascribed to the GM. In 2015, the total root density remained steady in SM-Control, whereas it increased by 2.9

Table 4 Estimation of the mean hydrodynamic parameters from the multi-tension disk infiltration experiments for GM and standard errors between parentheses in 2014 and 2015

Material	θ_r (−)	θ_s (−)	$|h_g|$ (cm)	n (−)	K_s (cm h^{-1})
2014					
GM Homécourt site	0.05	0.69	5.3 (0.2)	1.57 (0.06)	30.95 (8.45)
GM Angers site	0.05	0.77	2.95 (0.35)	1.48 (0.02)	26.35 (3.45)
2015					
GM Angers site	0.05	0.75	2.73 (0.36)	1.6 (0.3)	24.69 (8.98)

θ_s and θ_r are respectively the saturated and residual water contents, h_g the scale parameter for the water pressure head and K_s the saturated hydraulic conductivity

Table 5 Estimation of the mean hydrodynamic parameters from multi-tension disk infiltration experiments on structural materials (SM) and standard errors between parentheses in 2014 and 2015
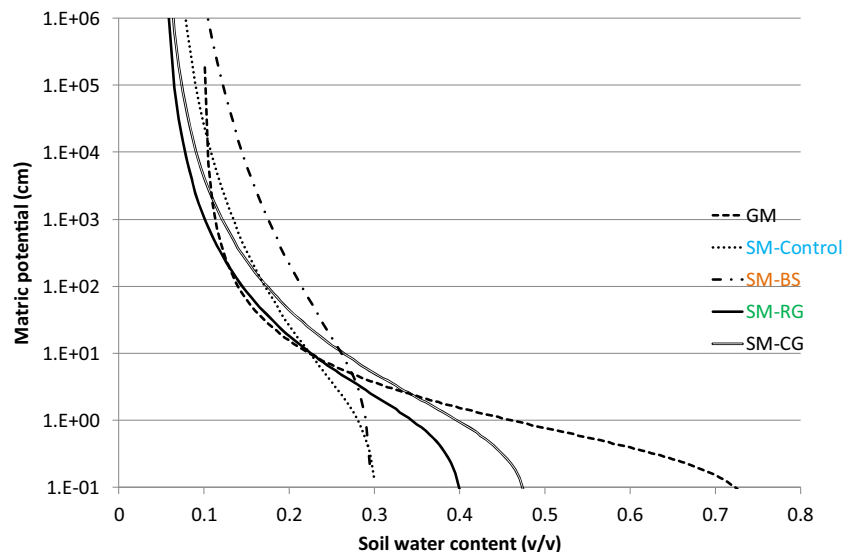
Material	θ_r (−)	θ_s (−)	$|h_g|$ (cm)	n (−)	K_s (cm h^{-1})
2014					
SM-Control	0.05	0.312	10.1 (2.5)	1.16 (0.08)	6.95 (5.95)
SM-BS	0.05	0.358	35.1 (28.1)	1.12 (0.06)	2.6 (0.9)
SM-RG	0.05	0.417	7.45 (1.75)	1.27 (0.13)	9.45 (2.75)
SM-CG	0.05	0.484	6.65 (0.65)	1.26 (0.02)	3.55 (1.55)
2015					
SM-Control	0.05	0.31	4.00 (0.57)	1.23 (0.05)	20.91 (10.49)
SM-BS	0.05	0.33	5.61 (2.25)	1.18 (0.02)	18.35 (6.24)
SM-RG	0.05	0.40	8.45 (4.11)	1.18 (0.05)	34.74 (4.01)

θ_s and θ_r are respectively the saturated and residual water contents, h_g the scale parameter for the water pressure head and K_s the saturated hydraulic conductivity

and 3.5 fold in SM-RG and SM-BS, respectively. Total root biomass values were 591, 963 and 1188 in SM-Control, SM-BS and SM-RG, respectively. Trees grown in SM-BS and SM-RG displayed the greatest root increase, particularly in SM-BS where root biomass was the lowest in 2014.

This same trend was observed for the aerial biomass (Table 8), wherein the SM-BS treatment had the lowest wood and leaf biomasses in 2014. Furthermore, the total aerial biomass was the highest in SM-Control (1445 g dw), followed by SM-RG (1065 g dw) and SM-BS (652 g dw). The total biomasses of SM-BS and SM-RG were respectively 2.2 and 1.3 times less than that of SM-Control. In 2015, the trees grown in SM-Control displayed the lowest aerial biomass (1595 g dw), 1.9 and 2.3 times as low as in SM-RG and SM-BS, respectively. For the trees grown in SM-RG, total biomass was 2.9 times as high in 2015 as in 2014, whereas it was 5.6 times as high in SM-BS.

3.3.2 Lawns

In order to assess the influence of the physical properties of prepared structural soil on vegetation development, the root distribution profile was measured on the GISFI lysimeter (Fig. 9). Based on this observation, 32.8 % of the total soil volume (1.85 m deep over 1 m^2) was colonized by roots. The root profile was clearly separated into three layers: (i) between 0 and 70 cm deep, the soil was fully rooted in both GM and SM-CG; (ii) between 72 and 162 cm deep, only SM-CG existed (settlement decreased the depth of the GM material) and root density gradually decreased with depth; (iii) below 164 cm, hardly any root was observed. The biomass was harvested on the GISFI lysimeter and, considering that both materials covered the same surface area (0.5 m^{-2}), dry biomass production was evaluated at respectively 80 and 60 g dw m^{-2} for GM and SM-CG.

4 Discussion

The originality of this study is based on an overall and dynamic monitoring of physical parameters (density, porosity, soil water retention, available water, soil aeration and hydraulic conductivity) to understand urban soil hydrodynamics. Such results were also interestingly associated with the evaluation of plant root development in order to assess the physical fertility of such artificial media.

4.1 The hydrodynamic properties of constructed urban soil

The main constraint in our study was the determination of the hydrodynamic properties of prepared structural soils without any soil core sampling for soil water retention or any

Fig. 7 Soil water retention curve of GM, SM-CG, SM-BS, SM-Control and SM-RG. [Volumetric water content (−) on the horizontal axis and pressure head (cm) on the vertical axis]

Fig. 8 Unsaturated hydraulic conductivity curves of GM, SM-CG, SM-BS, SM-Control and SM-RG as a function of **a** volumetric water content [−] and **b** pressure head
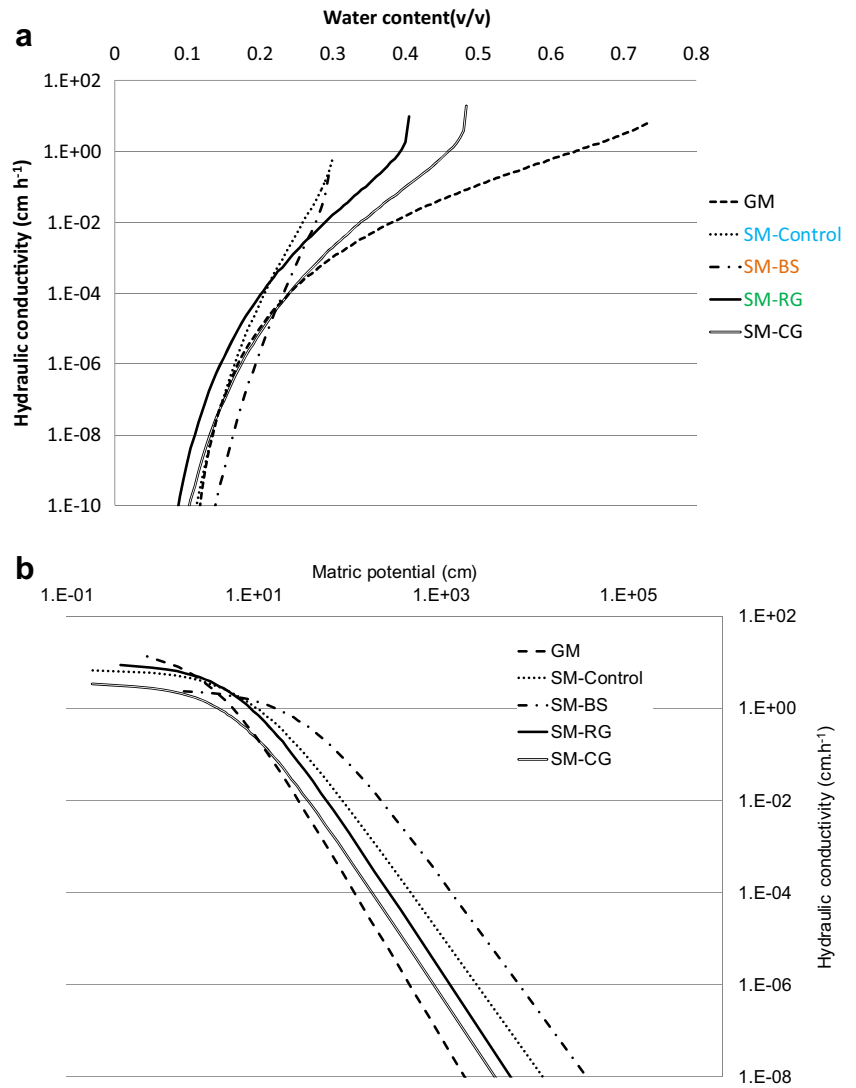
characterization of soil hydraulic conductivity curves, due to the high stone content that forbade core sampling. Producing

complete curves and their associated parameters became even more necessary when conducting water balance modeling and

Table 6 Physical properties indicators for all materials

Year	Material	Available soil water (mm cm^{-1})	Water stress delay (days)	Macroporosity (v/v)
	GM Angers site	3.09 (0.02) a	15.5 (0.76) a	0.32 (0.08) a
	GM Homécourt site	2.96 (0.04) a	12.35 (2.54) a	0.30 (0.04) a
2014	SM-Control	0.60 (0.14) b	6.65 (1.53) b	0.10 (0.04) b
	SM-BS	0.58 (0.09) b	6.33 (0.97) b	0.09 (0.06) b
	SM-RG	0.55 (0.05) b	6.09 (1.21) b	0.29 (0.09) b
	SM-CG	0.86 (0.02) b	31.97 (0.78) c	0.27 (0.01) b
	GM Angers site	2.85 (0.16) a	14.49 (1.5) a	0.27 (0.06) a
2015	SM-Control	0.50 (0.04) b	5.45 (0.45) b	0.16 (0.03) b
	SM-BS	0.66 (0.07) b	7.31 (0.74) b	0.16 (0.02) b
	SM-RG	0.77 (0.09) c	8.46 (0.94) d	0.18 (0.05) c

Numbers between parentheses are standard errors. Values without a common letter are significantly different according to a one-way ANOVA ($p < 0.05$)

Table 7 Tree root density (v/v) in each block of the three Angers site lysimeters in 2014 and 2015

|		A1	A2	A3	B1	B2	B3	C1	C2	C3	Total 2014	Total 2015
SM-Control	Layer I	1.0E−04	7.7E−05	6.4E−05	1.2E−04	*1.9E−02*	5.7E−04	8.4E−05	1.9E−04	9.0E−05	1.3E−03	1.5E−03
	Layer II	1.9E−04	2.5E−04	1.2E−04	4.4E−04	*8.9E−03*	2.9E−04	3.5E−04	7.2E−04	1.8E−04	2.3E−03	2.1E−03
	Layer III	1.5E−04	2.8E−04	3.2E−04	2.4E−04	4.8E−04	4.8E−04	2.8E−04	4.4E−04	5.4E−04	3.6E−04	7.0E−04
	Total 2014	1.5E−04	2.0E−04	1.7E−04	2.7E−04	9.6E−03	4.5E−04	2.4E−04	4.5E−04	2.7E−04	1.3E−03	−
	Total 2015	1.4E−04	2.8E−04	1.2E−04	3.5E−04	1.0E−02	2.6E−04	3.5E−04	6.6E−04	1.9E−04	−	1.4E−03
SM-BS	Layer I	6.7E−05	1.9E−04	6.1E−05	2.6E−04	*1.3E−02*	5.1E−04	9.4E−05	2.4E−04	8.8E−05	3.9E−04	2.0E−03
	Layer II	6.7E−05	3.8E−04	1.7E−04	3.7E−04	*1.5E−03*	3.3E−04	3.2E−04	2.6E−04	1.0E−04	1.7E−03	4.6E−03
	Layer III	0.0E + 00	4.7E−05	4.7E−05	6.1E−05	3.4E−05	4.7E−05	6.1E−05	2.7E−05	2.0E−05	3.8E−05	6.5E−04
	Total 2014	4.5E−05	2.0E−04	9.2E−05	2.3E−04	5.0E−03	3.0E−04	1.6E−04	1.8E−04	7.0E−05	6.9E−04	−
	Total 2015	2.3E−04	1.7E−04	4.3E−04	1.7E−03	1.5E−02	2.4E−03	5.4E−04	6.9E−04	6.0E−04	−	2.4E−03
SM-RG	Layer I	1.3E−04	1.6E−04	1.8E−04	1.0E−04	*1.4E−02*	1.5E−04	1.4E−04	1.2E−04	1.5E−04	1.0E−03	3.1E−03
	Layer II	2.3E−04	3.1E−04	2.4E−04	4.7E−04	*5.8E−03*	8.5E−04	2.7E−04	4.9E−04	2.9E−04	1.7E−03	2.9E−03
	Layer III	2.9E−04	3.5E−04	4.0E−04	3.4E−04	4.5E−04	3.3E−04	3.2E−04	3.4E−04	2.4E−04	3.4E−04	2.6E−03
	Total 2014	2.2E−04	2.7E−04	2.8E−04	3.0E−04	6.9E−03	4.4E−04	2.4E−04	3.2E−04	2.3E−04	1.0E−03	−
	Total 2015	9.9E−04	1.9E−03	8.5E−04	2.0E−03	1.6E−02	1.0E−03	8.9E−04	1.1E−03	6.7E−04	−	2.9E−03

Values in italics are the root density in the growing material (blocks I.B.2 and II.B.2)

predicting the sustainability of stony soil agronomic properties. Water infiltration experiments were preferred when performing *in situ* hydrodynamic characterization. Moreover, two experimental sites were used to conduct this study, and we can wonder whether climate conditions could have an effect on the constructed soils. We compared meteorological data in Homécourt and Angers sites for the 2013–2015 period. Cumulated rainfall during these 3 years was 2162 and 2139 mm for Angers and Homécourt sites, respectively. Thus, we cannot consider particular differences in water inputs. The annual mean air temperature was 12.8 and 11.3 °C in Angers and Homécourt, respectively. Such a difference should impact microbial processes such as organic matter decomposition. Considering a temperature factor correction such as proposed by Recous (1995) for organic matter dynamics modelling, Angers site factor correction would present a correction factor 1.2 times higher than Homécourt site. This factor is relatively low and temperature difference between sites should be neglected.

Table 8 Tree aerial biomass (in g dw) on the Angers site lysimeters in 2014 and 2015

Year	Treatment	Leaves	Wood	Total
2014	SM-Control	325.1	1119.6	1444.8
	SM-BS	190.3	461.7	652.1
	SM-RG	322.0	743.2	1065.3
2015	SM-Control	558.5	1006.3	1594.8
	SM-BS	1301.3	2324.1	3625.3
	SM-RG	1158.2	1915.0	3073.2

To our knowledge, such a complete approach has never been undertaken before. Grabosky et al. (2009) developed structural soils called Cornwell University (CU) Structural Soils, composed of 80 % of gravel with a 1.25–2.5 cm particle size. They only focused on soil water retention to calculate the soil water reservoir at two matric potentials corresponding respectively to the water holding capacity and soil water content at the wilting point. The CU-Structural Soil K_s value lays around 60 cm h^{-1}, i.e. 1.7 to 23 times higher than our values (Grasbosky et al. 2009). Compared to CU-Structural Soils, our materials were quite distinct in material composition: the
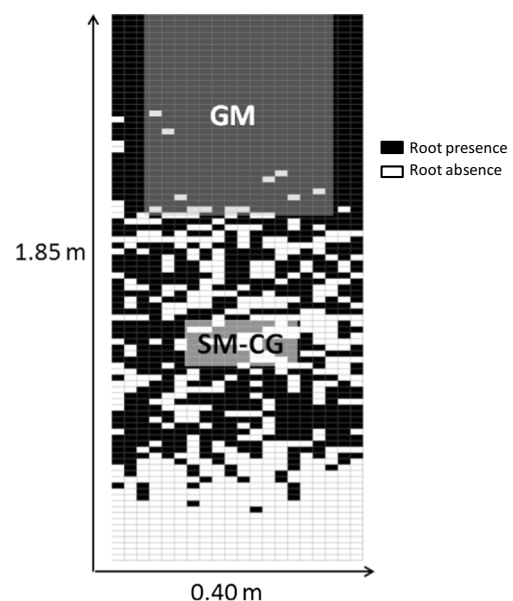
Fig. 9 Root distribution profile at the GISFI site in Homécourt

gravimetric ratio of coarse material was lower; 40 % of our materials had a particle size greater than 4 cm; different earth and organic materials were incorporated into our constructed soils; and the compaction procedure was unique. The presence of stones reduces the surface available for water infiltration and thus usually results in a decrease in infiltration rate (Ma et al. 2010). Nevertheless, the infiltration rate sometimes increases (Cousin et al. 2003) because of the creation of preferential pathways at the fine earth-stone interface (Zhou et al. 2009). The values obtained for saturated hydraulic conductivity were comparable to those measured for loamy or sandy-loamy soils (Van Genuchten 1980; Schaap et al. 2001), thus demonstrating the strong capacity of these constructed urban soils for water infiltration.

The hydrodynamic properties of growing media showed that it is a semi-permeable medium. It differed from structural material properties as a result of their higher organic matter content: GM contained 120 g kg^{-1} of organic matter, while SMs contained from 7.3 to 62 g kg^{-1}. Organic matter is well known for its high total porosity, ranging from 0.7 v/v for compost to 0.9 v/v for peat (Cannavo and Michel 2013; Cannavo et al. 2014), which in turn confers low dry bulk and specific densities, though with a highly saturated volumetric water content. Our findings confirm this general principle since the organic content of GM was far greater than that of the SMs (Table 3). The hydrodynamic parameters values obtained by infiltration experiments were in the same range than those obtained by Yilmaz and Dal (2015) with a similar GM packed in laboratory column and where hydrodynamic parameters were obtained using inverse modeling of a Wind method experiment.

Water retention and unsaturated hydraulic conductivity curves were quite similar for the four SMs, especially at low water content levels (except for the SM-BS water retention curve). This finding is probably due to the fact that as water content decreased, suction increased and the water remaining in the soil was more readily stored in the non-mineral fraction, which was essentially the same for all SMs (only the small organic fraction differed). The sole exception to this rule of thumb seems to have been SM-BS, which may pertain to the role of the (small) organic fraction of this material (sewage sludge) and its potentially inexplicable hydrodynamic behavior. The evolution of soil hydrodynamic parameters over time was noted at the Angers site. We demonstrated that globally speaking, these parameters remained stable between 2014 and 2015. Only K_s significantly increased in SMs for reasons mentioned below.

4.2 Vegetation growth capacity of constructed soils

Tree root measurements and root profile results are encouraging because they demonstrate that 1 or 2 years after planting, the trees and lawn were able to grow in soils solely constructed from wastes. This finding was confirmed by the plants' ability to develop roots that colonized the entire dedicated volume. As regards the lawn, root density was significantly higher in GM than in SM, which is consistent with their respective physical properties. Besides, vegetation development (i.e. root distribution and dry biomass) was thoroughly comparable to natural grasslands (Séré et al. 2008). In 2014, total tree root density was nearly 5 and 7 times less than the values given in Bartens et al. (2009) and Loh et al. (2003), respectively.

Urban soils dedicated to greening applications should have ASW for plants and MP values greater than 1 mm cm^{-1} and 0.2 v/v, respectively (Dexter 1988; Pagliai and Vignozzi 2002). While structural soils displayed good water infiltration capacity, the soil water reservoir for plant uptake was reduced due to a high stone content. All these materials had approximately the same mass ratios of fine minerals, stone, and organic matter. The high SAW (0.21 v/v at −316 cm water suction) in GM resulted from its high amount of exogenous organic matter and brick manufacturing waste water. Grabosky et al. (2009) found available water values ranging between 0.23 and 0.36 mm cm^{-1}, which is lower than our findings. The ASW for a natural loamy soil, with a soil bulk density around 1.35 g cm^{-3}, had a mean value of 1.3 mm cm^{-1} (Schaap et al. 2001). Compared to our stony soils, this value is 1.5 to 2.4 times as high as SMs in 2014. Cousin et al. (2003) demonstrated that ASW can be overestimated by 22–39 % when rock fragment are not taken into account and underestimated by 8–34 % when the volume of rock fragment is taken into account but not their retention properties. Indeed, stones are able to contribute to water retention depending on their bulk density and solid density (i.e. their total porosity) (Tetegan et al. 2011). In our study, stones presented contrasted total porosities, resulting in different stone water retention capacities. Track ballast, concrete waste and demolition rubble had water retention capacities (at −316 cm water suction) of 0.09, 0.14 and 0.19 v/v, respectively. Then, even if stone addition reduces the global ASW of the constructed soils, such stones contribute significantly in water storage.

The main consequence of such differences is to contrast the soil water autonomies of the various SM treatments, which had been particularly noteworthy for trees planted at the Angers site. Nevertheless, these results shall be considered by taking into account the small soil volume in the Angers site (i.e. 0.48 m^3), which is crucial in the soil autonomy calculation. In cities, pit plantations generally occupy at least 1–2 m^3 (Grabosky and Bassuk 1995; Lemaire and Sorin 1996). Even though these soils constructed from wastes offer rather attractive physical properties for tree growth, water demand should be monitored and irrigation could be required, especially during the first year of tree growth. More attention should be paid to macroporosity results because structural materials displayed lower values than recommended. SM-Control and SM-BS had very low MP values (≥0.1 v/v in 2014 and also in 2015). Finally, SM-RG was the only material that displayed

significant increases in K_s and SAW from 2014 to 2015. The very nature of organic wastes (i.e. sludge, composted or non-composted green waste) has a strong influence on organic matter transformation processes (i.e. degradation, mineralization) that can strongly influence parameters such as soil porosity.

Contrasted root growth and lawn development were observed as a function of treatment type. In 2014, SM-BS seemed to be less favorable to tree growth, whereas it supplied for the highest tree aerial biomass in 2015. Results were similar on SM-CG during the first year: ryegrass initially hardly settled and then reached high biomass production in the second year. The main hypothesis for root growth limitation may be the presence of redox spots observed over the lower part of the lysimeters in 2014 and disappeared in 2015. This result is consistent with previous observations on recent constructed soils (Séré et al. 2010). It appeared that the waste mixtures initially lacked structure, especially as far as pore connectivity is concerned. Consequently, there was a significant risk of water stagnation and anoxic conditions inside the constructed soils. As Technosols are submitted to an early pedogenesis–under the effects of vegetation, biological activity, and climate–soil structure improved and led to better vegetation development. On the opposite, despite the highest initial organic matter content in SM-Control (from 1.3 to 2.7 times more compared to others SMs), tree growth was limited. Although there was no excess or deficiency in macro and micro-nutrients, the soil pH of SM-Control was extremely low (Table 2).

5 Conclusions

The present study validates the capacity of Technosols made solely of wastes in order to support vegetation (trees and lawns). To achieve two major and complex urban soil functions, namely supporting vegetation and light traffic, these constructed soils were associated with a growing material and a structural material, featuring specific properties like a coarse texture that required developing an original methodology to obtain data on their physical properties, and more particularly their hydrodynamic properties. The primary advantage of this soil engineering approach is to demonstrate that rationally formulated artefacts (IUSS 2014) such as bricks, concrete, ballast, green waste or sewage sludge can lead to the implementation of multifunctional soils in cities. Moreover, they are capable of providing sustainable effective water infiltration conditions, a satisfactory level of water retention and favorable chemical conditions. As a consequence, trees developed better on constructed soils than on control structural material. However, attention should be paid to waste formulation and constructed soil implementation. The choice of organic wastes appeared crucial. Thus, we demonstrated that composted organic or sludge wastes are a good compromise for water retention and air availability as compared to non-composted green wastes. It also appears relevant to pre-cultivate some waste

mixtures before their implementation to improve the soil structure and avoid anoxic conditions.

Finally, stone addition as structural material up to 75 % in mass induced an efficient skeleton to avoid soil packing. Such a practice is currently undertaken in various French cities for tree plantation types, presenting successful results. So far it was not scientifically proven. Another measurement campaign will start in 2016 in Angers site to confirm the consistency of the soil hydrodynamic properties.

References

ADEME (2012) Les déchets- Chiffres Clés (Edition 2012)

Baetens JM, Verbist K, Cornelis WM, Gabriels D, Soto G (2009) On the influence of coarse fragments on soil water retention. Water Resour Res 45:W07408

Bartens J, Day SD, Harris JR, Wynn TM, Dove JE (2009) Transpiration and root development of urban trees in structural soil stormwater reservoirs. Environ Manag 44:646–657

Bartens J, Wiseman PE, Smiley ET (2010) Stability of landscape trees in engineered and conventional urban soil mixes. Urban For Urban Green 9:333–338

Böhm W (1979) Methods of studying root systems. Springer-Verlag, Berlin

Brakensiek DL, Rawls WJ (1994) Soil containing rock fragments: effects on infiltration. Catena 23:99–110

Cameira MR, Fernando RM, Pereira LS (2003) Soil macropore dynamics affected by tillage and irrigation for a silty loam alluvial soil in southern Portugal. Soil Till Res 70:131–140

Cannavo P, Michel JC (2013) Peat particle size effects on spatial root distribution, and changes on hydraulic and aeration properties. Sci Hortic 151:11–21

Cannavo P, Vidal-Beaudet L, Grosbellet C (2014) Prediction of long-term sustainability of constructed urban soil: impact of high amounts of organic matter on soil physical properties and water transfer. Soil Use Manag 30:272–284

Core Team R (2015) R: a language and environment for statistical computing. R Foundation for Statistical Computing, Vienna, Austria

Cousin I, Nicoullaud B, Coutadeur C (2003) Influence of rock fragments on the water retention and water percolation in a calcareous soil. Catena 53:97–114

Craul PJ (1999) Urban soils, applications and practices. Wiley, New York

Dexter AR (1988) Advances in characterization of soil structure. Soil Till Res 11:199–283

Djedjig R, Bozonnet E, Belarbi R (2013) Experimental study of the urban microclimate mitigation potential of green roofs and green walls in street canyons. Int J Low-Carbon Technol. doi:10.1093/ijlct/ctt019

Grabosky J, Bassuk N (1995) A new urban tree soil to safely increase rooting volumes under sidewalks. J Arboric 21:187–201

Grabosky J, Haffner E, Bassuk N (2009) Plant available moisture in stone-soil media for use under pavement while allowing urban tree root growth. Arboricult Urban For 35:271–278

Hanna K, Lassabatere L, Bechet B (2009) Zinc and lead transfer in a contaminated roadside soil: experimental study and modeling. J Hazard Mater 161:1499–1505

Huot H, Séré G, Charbonnier P, Simonnot MO, Morel JL (2015) Lysimeter monitoring as assessment of the potential for revegetation to manage former iron industry settling ponds. Sci Total Environ 526:29–40

IUSS Working Group WRB. World reference base for soil resources (2014) International soil classification system for naming soils and creating legends for soil maps. Report N°106. FAO, Rome

Kodesova R, Šimůnek J, Nikodem A, Jirku V (2010) Estimation of the dual permeability model parameters using tension disk infiltrometer and Guelph permeameter. Vadose Zone J 9:213–225

Lemaire F, Sorin X, (1996) Artificialisation du milieu de culture dans les espaces verts urbains. In: Les Colloques. La plante dans la ville, Angers (France), 5–7 Novembre 1996, INRA Ed., Angers, France, pp 247–256

Loh FCW, Grabosky JC, Bassuk NL (2003) Growth response of *Ficus benjamina* to limited volume and soil dilution in a skeletal soil container study. Urban For Urban Green 2:53–62

Ma D, Shao M, Zhang J, Wang Q (2010) Validation of an analytical method for determining soil hydraulic properties of stony soils using experimental data. Geoderma 159:262–269

Mallants D, Jacques D, Tseng PH, van Genuchten MT, Feyen J (1997) Comparison of three hydraulic property measurement methods. J Hydrol 199:295–318

Marquardt DW (1963) An algorithm for least-squares estimation of non-linear parameters. SIAM J Appl Math 11:431–441

Marshall RE Farahbakhsh K (2013) Systems approaches to integrated solid waste management in developing countries. Waste Management. ISBN: 0470999675

Morel JL, Schwartz Florentin, L. C (2005) Urban soils. Encyclopedia of soils in the environment, Elsevier, pp 202–208

Mualem Y (1976) A new model for predicting the hydraulic conductivity of unsaturated porous media. Water Resour Res 12:513–522

NF EN 933-1 (2012) Essais pour déterminer les caractéristiques géométriques des granulats - Partie 1: détermination de la granularité - Analyse granulométrique par tamisage

NF ISO 10390 (2005) Qualité du sol - Détermination du pH

NF ISO 11263 (1995) Qualité du sol - Dosage du phosphore - Dosage spectrométrique du phosphore soluble dans une solution d'hydrogénocarbonate de sodium

NF ISO 13878 (1998) Qualité du sol - Détermination de la teneur totale en azote par combustion sèche ("analyse élémentaire")

NF ISO 14235 (1998) Qualité du sol - Dosage du carbone organique par oxydation sulfochromique

NF P94-054 (1991) Sols : reconnaissance et essais - Détermination de la masse volumique des particules solides des sols - Méthode du pycnomètre à eau

Nielsen TS, Hansen KB (2007) Do green areas affect health? Results from Danish survey on the use of green areas and health indicators. Health Place 13:839–850

Novak V, Knava K, Simunek J (2011) Determining the influence of stones on hydraulic conductivity of saturated soils using numerical method. Geoderma 161:177–181

Ojeda G, Mattana S, Bonmati M, Woche SK, Bachmann J (2011) Soil wetting-drying and water-retention properties in a mine-soil treated with composted and thermally-dried sludges. Eur J Soil Sci 62:696–708

Pagliai M, Vignozzi N (2002) Soil pore system as an indicator of soil quality. In: Pagliai M, Jones R (eds) Sustainable soil management for environmental protection. Soil physics aspects. Catena, Reiskirchen, pp 71–82

Poesen J, Lavee H (1994) Rock fragments in top soils: significance and processes. Catena 23:1–28

Ramos TB, Goncalves MC, Martins JC, van Genuchten MT, Pires FP (2006) Estimation of soil hydraulic properties from numerical inversion of tension disk infiltrometer data. Vadose Zone J 5:684–696

Recous S. (1995) Réponse des matières organiques des sols aux changements atmosphériques globaux. II. Effet de la température sur la minéralisation d'un résidu végétal (maïs) et de la matière organique des sols. In: Perrier A, Saugier B (eds) Dossiers de l'environnement de l'INRA n°8, Paris, pp 81–86

Rokia S, Séré G, Schwartz C, Deeb M, Fournier F, Nehls T, Damas O, Vidal-Beaudet L (2014) Modelling agronomic properties of Technosols constructed with urban wastes. Waste Manag 34:2155–2162

Sarah P (2002) Spatial patterns of soil moisture as affected by shrubs, in different climatic conditions. Environ Monit Assess 73:237–241

Schaap MG, Leij FJ, van Genuchten MT (2001) ROSETTA: a computer program for estimating soil hydraulic parameters with hierarchical pedotransfer functions. J Hydrol 251:163–176

Schwartz RC, Evett SR (2002) Estimating hydraulic properties of a fine textured soil using a disc infiltrometer. Soil Sci Soc Am J 66:1409–1423

Seber GAF, Wild CJ (2003) Nonlinear regression. Wiley, New York

Séré G, Ouvrard S, Magnenet V, Pey B, Morel JL, Schwartz C (2012) Predictability of the evolution of the soil structure using water flow modeling for a constructed technosol. Vadose Zone J 11 0-0

Séré G, Ouvrard S, Schwartz C, Renat JC, Morel JL (2008) Soil construction: a step for ecological reclamation of derelict lands. J Soils Sediments 8:130–136

Séré G, Schwartz C, Ouvrard S, Renat JC, Watteau F, Villemin G, Morel JL (2010) Early pedogenic evolution of constructed Technosol. J Soils Sediments 10:1246–1254

Šimůnek J, van Genuchten MT (1996) Estimating unsaturated soil hydraulic properties from tension disc infiltrometer data by numerical inversion. Water Resour Res 32:2683–2696

Simůnek J, van Genuchten MT (1997) Estimating unsaturated soil hydraulic properties from multiple tension disc infiltrometer data. Soil Sci 162(6):383–398

Šimůnek J, Angulo-Jaramillo R. Schaap MG, Vandervaere JP, van Genuchten MT (1998) Using an inverse method to estimate the hydraulic properties of crusted soils from tension-disc infiltrometer data. Geoderma 86:61–81

Šimůnek J, van Genuchten MT, Sejna M (2008) Development and applications of the HYDRUS and STANMOD software packages and related codes. Vadose Zone J 7:587–600

Tardieu F, Manichon H (1986) Caractérisation en tant que capteur d'eau de l'enracinement du maïs en parcelle cultivée. Agronomie 6:345–354

Tetegan M, Nicoullaud B, Baize D, Bouthier A, Cousin I (2011) The contribution of rock fragments to the available water content of stony soils: proposition of new pedotransfer functions. Geoderma 165:40–49

Ugolini FC, Corti G, Agnelli A, Certini G (1998) Under and overestimation of soil properties in stony soils. 16th World Congress of Soil Science. Montpellier, France

Urban J (2013) Two different approaches to improve growing conditions for trees. Arboricultural Consult 46:5–12

van Genuchten MT (1980) A closed form equation for predicting the hydraulic conductivity of unsaturated soils. Soil Sci Soc Am J 44:892–898

Yilmaz D, Dal L (2015) Hydraulic properties estimation of an experimental urban soil column constructed with waste brick and compost. Int J Pure Appl Sci 1:9–15

Yilmaz D, Lassabatere L, Deneele D, Angulo-Jaramillo R, Legret M (2013) Influence of carbonation on the microstructure and hydraulic properties of a basic oxygen furnace slag. Vadose Zone J. doi:10.2136/vzj2012.0121

Yuan HP, Shen LY (2011) Trend of the research on construction and demolition waste management. Waste Manag 31:670–679

Zhou BB, Shao MA, Shao HB (2009) Effect of rock fragments on water movement and solute transport in a loess plateau soil. C R Géosci 341:462–472